J Mater Sci (2010) 45:2868–2873
DOI 10.1007/s10853-010-4276-z

Electrical and magnetic properties of copper tellurite glasses

P. Sandhya Rani · R. Singh

Received: 27 October 2009 / Accepted: 25 January 2010 / Published online: 9 February 2010

Abstract The glasses of composition $(100 - x)TeO_2$–$xCuO$ ($x = 10, 20, 30, 40, 50$ mol%) were prepared by melt quenching method. Differential Scanning Calorimetry (DSC), DC conductivity, Electron Spin Resonance (ESR), and magnetization measurements were undertaken on the glass samples. The glass-transition temperature, T_g, decreases and the thermal stability ($\Delta T = T_o - T_g$) increases with the increase in CuO content. The electrical conduction in these glasses is due to polaron hopping mechanism in the adiabatic regime. The ESR spectra of the $x = 10$ glass consists of a broad symmetrical line characteristic of Cu^{2+} clusters. The ESR signal linewidth increases and intensity decreases drastically with increase in CuO content from 10 to 20 mol%. No ESR signal could be observed for the glass samples with $x \geq 40$. The absence of EPR signal is ascribed to antiferromagnetic interactions between the Cu^{2+} clusters. The magnetization measurements indicate all the samples to be in paramagnetic state. The *M–H* plots show a small hysteresis loop in the low-field region. These studies indicate the coexistence of antiferromagnetic (AFM) as well as ferromagnetic (FM) interactions between Cu^{2+} ions in these glasses. The significant change in the properties of the glass at $x = 20$ is ascribed to the structural changes caused by CuO in the glass matrix.

Introduction

The tellurite glasses are technologically important since they are known to have low melting temperature, high chemical stability, high homogeneity, high refractive index, high dielectric constant, and high transmittance from ultraviolet to near infrared. The TeO_2-based glasses have been widely studied due to their possible applications in infrared and optoelectronic devices [1–4]. The addition of TM ions to these glasses shows semi conducting properties and finds applications in switching and memory devices [5, 6]. A number of studies on the structure of tellurite glasses [7–10] have revealed that tellurite glasses consist of TeO_4 trigonal bi-pyramids, deformed TeO_4 groups, TeO_{3+1} units, and TeO_3 trigonal pyramids or a combination of these polyhedra. The glass formation range in binary TeO_2–MO (MO = 3d transition metal (TM) oxide-like V_2O_5, Fe_2O_3, etc.) composition has been reported [11]. There are few studies in literature on thermal studies of TM-ion-containing tellurite glasses [12–14]. TM ions characterized by a partially filled d shell can frequently exist in a number of oxidation states leading to the semi-conducting behavior of these glasses via electron transfer from ions in a lower valence state to those in a higher valence state. The electrical conductivity data on TM-ion-containing glasses is generally explained by small-polaron theory [15, 16]. Structural, electronic, optical, magnetic, and mechanical properties of these glasses depend upon the relative ratio of the different valence states of the TM ions present [17–21]. In order to account for the effect of these valence states on the structure and properties of these glasses, it is important to control and measure the ratios of the TM ion concentration in the different valence states of these oxide glasses. A number of studies on TeO_2–CuO glasses are reported in the literature [22–24]. In this article, we present a number of studies including Differential Scanning Calorimetry (DSC), DC conductivity, electron spin resonance (ESR), and magnetization on wide composition of $(100 - x)TeO_2$–$xCuO$

P. Sandhya Rani · R. Singh (✉)
School of Physics, University of Hyderabad,
Central University P.O., Hyderabad 500046, India
e-mail: rssp@uohyd.ernet.in

(where $10 \leq x \leq 50$ mol%) glasses. These studies have shown a clear dependence of various properties on the glass composition. These studies have also indicated that the antiferromagnetic (AFM) as well as ferromagnetic (FM) interactions between Cu^{2+} ions coexist in the glass matrix.

Experimental procedure

All glass samples of composition $(100 - x)TeO_2$–$xCuO$ (x mol%), where $x = 10, 20, 30, 40, 50$ were prepared by melt quenching method under identical conditions to minimize the effect of preparation conditions on the synthesized glasses. Glasses were characterized for their amorphous nature by XRD. Thermal studies were carried out using DSC using Model TA DSC 2010 by recording nonisothermal plots, in which the sample is heated at a constant rate and the change in heat with respect to an empty reference pan is measured. The small bulk pieces of different glass samples weighting 4–6 mg were used to avoid the effect of grain size. The bulk samples were run for DSC scans in temperature range from RT to 600 °C at heating rate of 10 °C/min. The temperature-dependent DC conductivity measurements were carried out on the disk-shaped glass samples using a Keithley electrometer Model 617. The ESR spectra of the samples were recorded on Joel X-Band ESR spectrometer in the temperature range 120–300 K. The magnetization studies were done using Lake Shore Cryotronics Magnetometer model 7400.

Results and discussions

DSC studies

The thermograms for various samples recorded at heating rate of 10 °C/min are shown in Fig. 1. Most of the samples show a well-defined sharp DSC crystallization peak indicating a uniform amorphous phase in the samples. Two characteristic temperature regions are evident in the DSC thermograms. The first one corresponds to the glass-transition region (endothermic reaction) and the other to the crystallization region (exothermic reaction). The glass-transition temperature T_g has been defined as the temperature, which corresponds to the intersection of the two linear portions adjoining the transition elbow of the DSC trace in the endothermic direction. Table 1 lists glass-transition temperature, T_g, crystallization onset temperature, T_o, crystallization peak temperature, T_p, and thermal stability ($\Delta T = T_o - T_g$). T_g decreases and ΔT increases with the increase in CuO content. There is a sharp increase in ΔT as CuO content increases from 20 to 30 mol%.

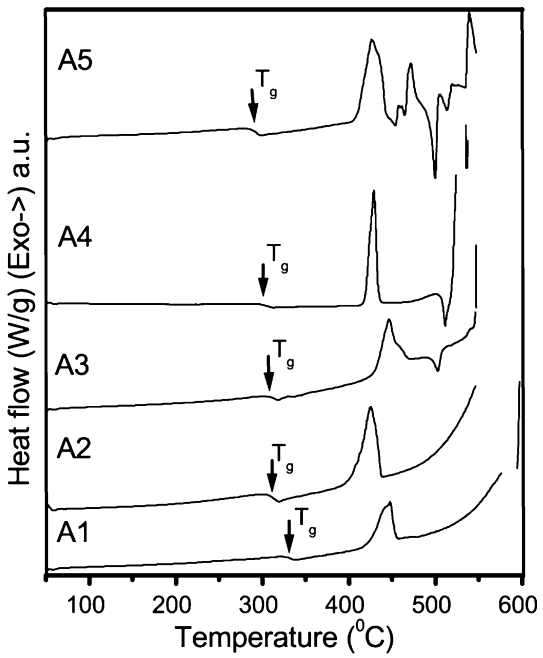

Fig. 1 DSC thermograms of copper tellurite glass samples

Table 1 Thermal parameters for various compositions of $(100 - x)TeO_2$–$xCuO$ glasses

Samples	Composition (x)	T_g (°C)	T_o (°C)	T_p (°C)	ΔT (°C)
A1	10	332	418	442	86
A2	20	310	398	426	88
A3	30	310	424	446	114
A4	40	302	417	428	115
A5	50	286	408	427	122

In the case of samples A1, A2, and A3 more than one exothermic peak indicating different stages of crystallization are observed.

DC conductivity studies

Figure 2 shows $\log_{10}(\sigma)$ versus $1000/T$ for various glasses of $(100 - x)TeO_2$–$xCuO$ compositions. The conductivity increases by almost two-order of magnitude as CuO content increases from 10 to 20 mol%. With further increase in CuO the conductivity increase at a slower pace. The $\log_{10}(\sigma)$ versus $1/T$ plot is linear in the high temperature range and it departs from linearity with decrease in temperature. The value of conductivity in the present samples is almost 2–3 orders of magnitude lower than reported by other workers on the same compositions [22]. The electrical conductivity data in oxide glasses containing TM oxide [18, 22] has been widely analyzed in view of small-polaron model given by Mott [15] and Austin and Mott [16]. According to this model, the conduction in TM-ion-

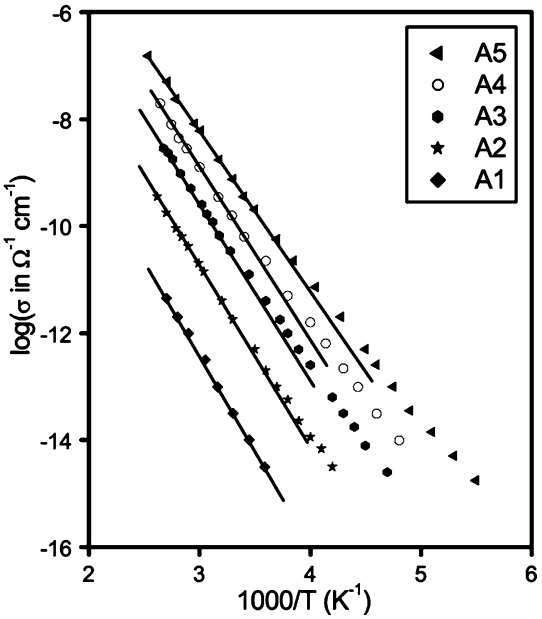

Fig. 2 Log_{10} (σ) versus 1000/T for various glass compositions

containing glasses takes place by thermally assisted small-polaron hopping from low valence state to the high valence state of the TM ion (like between Cu^{+} and Cu^{2+} ions). In the high temperature range, i.e., $T > \theta_D/2$, the DC conductivity is due to small-polaron hopping among the nearest neighbors and in the nonadiabatic regime it is given by

$$\sigma = \frac{v_0 N e^2 R^2}{kT} c(1-c) e^{-2\alpha R} e^{-W/kT} \quad (1)$$

where σ is the conductivity at temperature T, v_0 is the phonon frequency, c is the ratio of concentration of the TM ions in the low valence state to the total number of TM ions N, R is the average hopping distance, α is the electron-wave-function decay constant of the 3d electron wave function, and W is the activation energy for conduction. Assuming a strong electron–lattice interaction, Austin and Mott [16] have shown that

$$W = W_H + \frac{1}{2}W_D \text{ for } T > \theta_D/2, \quad W = W_D \text{ for } T < \theta_D/4, \quad (2)$$

where W_H is the polaron-hopping energy and W_D is the disorder energy arising from energy differences of the neighboring sites. $\theta_D \approx h\, v_0/k$ is the Debye temperature and v_0 the phonon frequency of the material. The tunneling term exp $(-2\alpha R)$ in Eq. 1 reduces to unity if polaron hopping is in the adiabatic regime and the conduction is mainly controlled by the activation energy W. This model predicts an appreciable departure of linearity in a $\log_{10}$ (σ) versus 1/T plot below a temperature $T = \theta_D/2$ indicating decrease in activation energy with the decrease in temperature. The continuous curvature observed $\log_{10}$ (σ) versus 1/T plot indicative of the decrease in activation with decrease in temperature. The estimated θ_D value is in the range of 200–250 K. The estimation of W_D requires data below 50 K. Because of very high resistivity of the samples in the low temperature range, the data could not be taken below 140 K.

Table 2 Electrical parameters of various glass compositions

Samples	σ at 300 K (Ω^{-1} cm^{-1})	W (eV)
A1	3.14×10^{-14}	0.72
A2	1.77×10^{-12}	0.67
A3	3.37×10^{-11}	0.65
A4	1.54×10^{-10}	0.64
A5	7.38×10^{-10}	0.61

The W values estimated from the linear fits of the high temperature data for various glasses are listed in Table 2. The glass having the highest conductivity has the lowest activation energy. This is consistent with Eq. 1, but the variation in the pre-exponential term might be present and can lead to deviations of the experimental data from the equation. A $\log_{10}$ (σ) versus W plot at a high temperature, say 305 K can ascertain the variation in the pre-exponential term. Figure 3 shows such a plot to be a straight line. This shows that the pre-exponential term of Eq. 1 inclusive of $e^{-2\alpha R}$ is virtually constant and W appears to dominate the factors which determine the conductivity.

The nature of polaron hopping whether it is in the adiabatic or nonadiabatic regime can be ascertained from $\log_{10}$ (σ) versus W plot at a fixed temperature T for glasses of different compositions [18, 19]. The estimated temperature

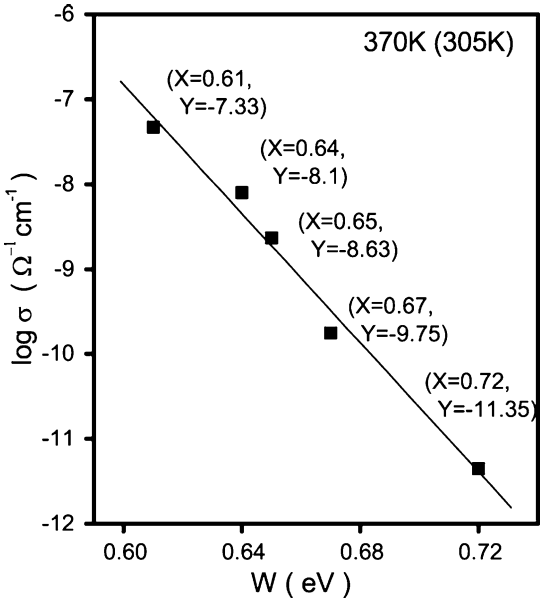

Fig. 3 Plot of the $\log_{10}$ (σ) versus W for various glass compositions

T_c from the slope of such a plot will be close to T if the hopping is in the adiabatic regime [i.e., $e^{-2\alpha R} = 1$ in Eq. 1] and will be different from T if the hopping is in the nonadiabatic regime and the term $e^{-2\alpha R}$ in Eq. 1 cannot be ignored. The temperature T_c (within brackets) is very much closer from the temperature at which the $\log_{10}(\sigma)$ is plotted against W in Fig. 3. This further supports that the tunneling term $e^{-2\alpha R}$ in Eq. 1 can be ignored and the conduction in the present glasses is in the adiabatic regime.

ESR studies

The ESR spectra of TeO_2–CuO glasses are shown in Fig. 4. A well-defined resonance at $g \approx 2.2$ with peak to peak linewidth (ΔH) of $\sim$450 G and no hyperfine structure is observed for the $x = 10$ sample The (ΔH) increases and the intensity of the resonance decreases as the CuO content increases. Very weak ESR signal is observed in sample with $x = 30$. No ESR signal could be observed for sample with $x = 40$ and 50. The asymmetry of the resonance line indicates that ESR spectra for $x = 10$ is a superposition of two signals; one due to isolated Cu^{2+} ions in axial neighborhood and second a larger ESR signal from interacting Cu^{2+} ion coupled as clusters by exchange coupling. The decrease in intensity for $x > 20$ mol% is due to increasing contribution from Cu^{2+} ion spins coupled in antiparallel configuration by super exchange-type interactions. The increase in CuO content increases the concentration of antiferromagnetically coupled Cu^{2+} ion leading to the line broadening and disappearance of ESR signal. The decrease in ESR signal intensity at high concentration of CuO in copper tellurite glasses is also reported by Criocas et al. [23] and is attributed to the presence of Cu^{+} and Cu^{2+} ions in the system, larger spatial disorder or the magnetic coupling between the ions. The spatial disorder may lead to wide distribution in Cu–O–Cu bond angles leading to ferromagnetic coupling also between Cu^{2+} ions. This however cannot be observed by ESR. The magnetization data indicate the existence of ferromagnetic coupling between Cu^{2+} ions.

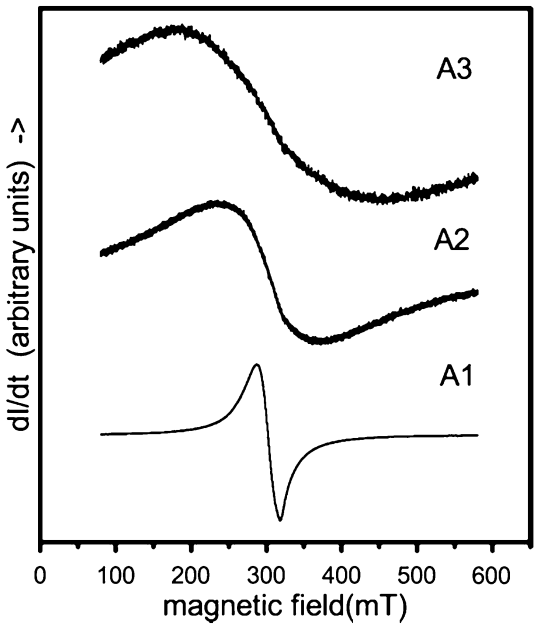

Fig. 4 ESR spectra for the glass samples at 123 K

Magnetization studies

Figure 5 shows the magnetization versus field for various glass samples. A small hysteresis loop in the low-field region is observed for all samples indicating the existence of ferromagnetic cluster formation in the glass matrix. Figure 6 shows the M versus H plots for various samples recorded in the low-field region.

The magnetization per unit field, molar curie constant, C_M, and the effective magnetic moments, μ_{eff}, are calculated and listed in Table 3. The μ_{eff} values are estimated using the relation $\mu_{eff} = 2.828(C_M/x)^{1/2}$ assuming that all copper ions introduced in the sample contribute to the magnetic moment of glass. Except for the sample with $x = 20$, the μ_{eff} values obtained for all samples are lower than the magnetic moment of the free ion ($\mu_{Cu}^{2+} = 1.73\mu_B$) indicating the presence of both Cu^{2+} and Cu^{+} ions in these glasses. Cu^{+} ions are diamagnetic in nature and do not contribute to magnetic moment. Using the relation $\mu_{Cu}^{2+} = 2.828(C_M/y)^{1/2}$, we

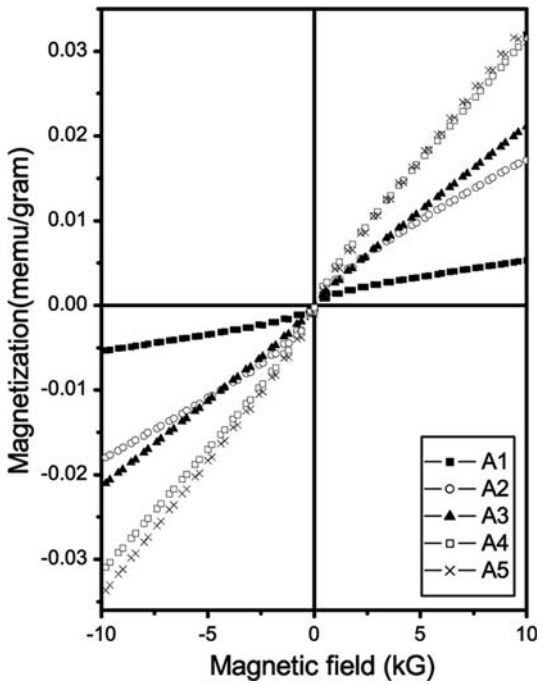

Fig. 5 Magnetization versus field for various copper tellurite glass samples

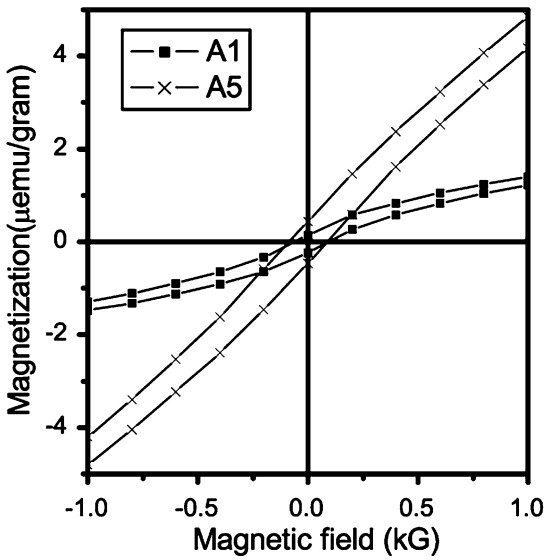

Fig. 6 *M* versus *H* in low-field region for various copper tellurite glass samples

Table 3 Magnetic parameters for the copper tellurite glasses

Samples	*M*/*H* (emu/mol) × 10^{-4}	C_M (emu/mol) × 10^{-2}	μ_{eff} μ_B	*y* (mol%)
A1	0.864	2.592	1.439	7
A2	2.556	7.668	1.751	20
A3	2.888	8.664	1.519	23
A4	4.03	12.091	1.555	32
A5	4.015	12.046	1.388	32

estimated to a first approximation the molar fraction of the Cu^{2+} ions (*y*) that contribute to the magnetic moment and listed in Table 3. It is observed that the molar fraction of the Cu^{2+} is equal to the CuO molar faction only in case of sample with $x = 20$ mol%. For other compositions, the molar fraction of the Cu^{2+} is lower when compared to the molar faction of CuO in the vitreous samples. The concomitant presence of monovalent and divalent copper ions is reported in copper containing tellurite glasses [19, 21, 24].

The present study shows that as CuO increases from 10 to 20 mol% there is a sudden change in the properties of glass followed by gradual variation with further increase in CuO content. These changes may be related to the structural changes in the glass matrix as CuO content increase. The TeO_2-rich glasses are characterized by TeO_4 building units. Both Te–O_{ax} axial bonds in the TeO_4 polyhedra are strongly dynamic and easily attacked by the modifier. When a modifier oxide is introduced in the glass matrix, one of the Te–O_{ax} bonds in TeO_4 polyhedra undergoes elongation. The introduction of a modifier in the binary glass leads to a $TeO_4 \rightarrow TeO_{3+1}$ transition. The number of TeO_{3+1} units is limited by modifier addition. With increase in modifier content the TeO_{3+1} units transform into TeO_3 and TeO_2 units. The glasses with low modifier content consist of a continuous random network constructed by sharing corners of TeO_4 trigonal bipyramids and TeO_{3+1}. The IR study by Dimitriev et al. [9] shows that both the 3- and the 4-coordinated tellurite polyhedra are simultaneously formed in tellurite glass. So, it seems quite plausible to assume that in CuO–TeO_2 glass 4-coordinated polyhedra are transformed into 3-coordinated ones with the increase of CuO modifier. As modifier content increases from 10 to 20 mol%, the TeO_3 trigonal pyramids having nonbridging oxygen spread to the whole network giving rise to high thermal stability to the glass network. The formation of Te–O–Cu and Cu–O–Cu bonds also takes as CuO content increases. The Cu–O–Cu bond is responsible for antiferromagnetically (AFM) and ferromagnetically (FM) coupled clusters in the glass matrix which increase the thermal stability and conductivity of the glass. Increase in CuO content increases the concentration of Cu–O–Cu bonds leading to formation of CuO-rich regions in the glass matrix as reported by Criocas et al. [23].

Conclusions

The glasses of composition $(100 - x)TeO_2$–$xCuO$, where $x = 10, 20, 30, 40, 50$ were prepared by melt quenching method. DSC, DC conductivity, ESR, and magnetization measurements were undertaken on the glass system. The glass-transition temperature decreases and the thermal stability increases with the increase in CuO content in the glass system. The electrical conduction in these glasses is due to polaron hopping mechanism in the adiabatic regime. The ESR spectra of the $x = 10$ glass consists of a broad symmetrical line with no hyperfine splitting is characteristic of Cu^{2+} clusters. The linewidth of the ESR signal increases with increase in CuO content. The signal intensity decreases drastically with increase in CuO content. No ESR could be observed for the glass samples with $x = 40$ and 50. The loss of ESR signal may be due to antiferromagnetic coupling between the Cu^{2+} clusters. The magnetization measurements indicate all the samples to be in paramagnetic state. The *M*–*H* plots show a small hysteresis loop in the low-field region. These studies indicate that the antiferromagnetic (AFM) as well as ferromagnetic (FM) interactions between Cu^{2+} ions coexist in the glass matrix.

The significant change in the properties of the glass at $x = 20$ is ascribed to the structural changes caused by CuO in the glass matrix.

Acknowledgement One of the authors SRP gratefully acknowledges the award of Junior Research Fellowship under CAS programme of School of Physics, University of Hyderabad.

References

1. Ovcharenko N, Yakhkind A (1968) Opt Mech Prom 3:47
2. Lines ME (1991) J Appl Phys 69:6876
3. Kim SH, Yoko T, Sakka S (1993) J Am Ceram Soc 76:2486
4. Wang JS, Vogel EM, Snitzer E (1994) Opt Mater 3:187
5. Gateff E, Dimitriev Y (1979) Philos Mag 40:233
6. Chung C, Mackenzie J (1980) J Non-Cryst Solids 42:357
7. Brady GW (1957) J Chem Phys 27:300
8. Neov S, Kozhukharov V, Gerasimova I, Krezhov K, Sidzhimov B (1979) J Phys C 12:2475
9. Dimitriev Y, Dimitriev V, Arunaudov M (1983) J Mater Sci 18:1353. doi:10.1007/BF01111954
10. Burger H, Kneipp K, Hobert H, Vogel W, Kozhukharov V, Neov S (1992) J Non-Cryst Solids 151:134
11. Kozhukharov V, Marinov M, Grigorova G (1978) J Non-Cryst Solids 28:429
12. Singh R (1987) J Phys D 20:548
13. Bahgat AA, Shaltout II, Abu-Elazm AM (1992) J Non-Cryst Solids 150:179
14. Chowdari BVR, Tan KL, Ling Fang (1998) Solid State Ion 113–115:711
15. Mott NF (1968) J Non-Cryst Solids 1:1
16. Austin G, Mott NF (1969) Adv Phys 18:41
17. Ardelean I, Ilonca G, Peteanu M (1982) J Non-Cryst Solids 51:389
18. Singh R, Chakravarthi JS (1997) Phy Rev B 55:5550
19. Singh R, Chakravarthi JS (1995) Phys Rev B 51:16396
20. Ardelean I, Filip S (2003) J Optoelectron Adv Mater 5:157
21. Ardelean I, Ciceo Lucacel R (2005) Phys Chem Glasses 46:491
22. Hassan MA, Hogarth CA (1988) J Mater Sci 23:2500. doi:10.1007/BF01111908
23. Criocas F, Mendiratta SK, Ardelean I, Valente MA (2001) Eur Phys J B 20:235
24. Khattak GD, Mekki A, Wenger LE (2004) J Non-Cryst Solids 337:174